Robust Cooperative Exploration With a Switching Strategy

Article *in* IEEE Transactions on Robotics · August 2012

DOI: 10.1109/TRO.2012.2190182

CITATIONS
68

READS
103

2 authors:

Wencen Wu
San Jose State University
52 PUBLICATIONS **521** CITATIONS
SEE PROFILE

Fumin Zhang
Georgia Institute of Technology
245 PUBLICATIONS **3,930** CITATIONS
SEE PROFILE

Robust Cooperative Exploration with a Switching Strategy

Wencen Wu, *Student member, IEEE,* Fumin Zhang, *Member, IEEE,*

***Abstract*—Biological inspirations lead us to develop a switching strategy for a group of robotic sensing agents searching for a local minimum of an unknown noisy scalar field. Starting with individual exploration, the agents switch to cooperative exploration only when they are not able to converge to a local minimum at a satisfying rate. We derive a cooperative H_∞ filter that provides estimates of field values and field gradients during cooperative exploration, and give sufficient conditions for the convergence and feasibility of the filter. The switched behavior from individual exploration to cooperative exploration results in faster convergence, which is rigorously justified by the Razumikhin theorem, to a local minimum. We propose that the switching condition from cooperative exploration to individual exploration is triggered by a significantly improved signal-to-noise ratio (SNR) during cooperative exploration. In addition to theoretical and simulation studies, we develop a multi-agent test-bed and implement the switching strategy in a lab environment. We have observed consistency of theoretical predictions and experimental results, which are robust to unknown noises and communication delays.**

***Index Terms*—Path Planning for Multiple Mobile Robot Systems, Sensor Networks, Motion Control, Cooperative Exploration**

I. Introduction

The main goal of cooperative exploration is to deploy a group of robotic sensing agents to explore an unknown scalar field efficiently and adaptively [1]–[7]. In typical scenarios, a cooperative group of agents are expected to perform better than a single agent [8]–[10]. However, increasing the number of agents results in rising cost, communication delay, and computational complexity. Therefore, the exploration behavior of each agent does not have to be fixed. Biologists have observed switching between individual and cooperative behaviors in certain species of fish [11]. It is conjectured that fish in a group collaborate with each other when they are not confident with the information gathered individually. A switching behavior model based on the level of confidence of individual fish has been studied. Simulation results in [11] show striking similarities to real fish data.

Inspired by the results in [11], we consider an exploration mission where multiple sensing agents search for a local minimum of an unknown scalar field. The major difference between our work and the biological results [11] is that we will not use the "level of confidence" directly since it is difficult to measure confidence of engineering systems. Instead, we propose two switching conditions that are related to the speed of convergence and the signal-to-noise ratio (SNR) [12], [13]. In this paper, we provide detailed explanation and proof for the strategy and additional experimental and simulation results. We assume that each agent has a finite memory length, and keeps exploring the field individually if it is guaranteed to locate a local minimum at a convergence rate that is compatible with its memory length. Based on the Razumikhin theorem, which was originally developed for verifying the stability of time-delay systems [14]–[16], we introduce sufficient conditions for a sensing agent with a given memory length to converge to a local minimum. The sufficient conditions then serve as switching conditions from individual exploration to cooperative exploration. If the sufficient conditions are violated, the convergence rate will not be guaranteed, then agents will start cooperative exploration. Shortly after cooperative exploration is started, each agent will compute a SNR and share it with all agents to compute an averaged SNR, which will be memorized by each agent. During the cooperative exploration, the averaged SNR will be updated and compared to the memorized SNR. When the current averaged SNR is significantly better than the memorized SNR, the agents switch back to individual exploration.

There are several successful extremum seeking algorithms in the literature [17]–[22]. Source seeking missions with one vehicle [18], [23]–[27] and groups of vehicles [2], [10], [20], [28]–[37] have been investigated. Compared to those algorithms, our strategy offers a novel aspect that focuses on the switching between individual and cooperative exploration. The switching conditions can be combined with existing exploration strategies to allow balanced performance between individual and cooperative exploration.

We have also derived a cooperative H_∞ filter that allows the field being explored to be corrupted by unknown noises. This is closer to real world applications than the Gaussian noise assumption in most literature. The cooperative H_∞ filter is constructed in the cooperative exploration phase to give estimated field values and gradients at the formation center. The H_∞ filter differs from the Kalman filter in that it does not require the knowledge of noise properties except that the noises are assumed to have bounded power, while the Kalman filter assumes the noises to be Gaussian. Therefore, the H_∞ filter is robust to possibly non-Gaussian noises [38]–[42]. An important constraint of the H_∞ filter is that the existence of the filter requires the fulfillment of a set of feasibility conditions, which further creates constraints on the exploration behaviors for the cooperative agent formation. Convergence analysis of H_∞ filters has been performed in literature [43]–

The research is supported by ONR grants N00014-08-1-1007 and N00014-09-1-1074, and NSF grants ECCS-0841195, ECCS-0845333(CAREER) and CNS-0931576. Wencen Wu and Fumin Zhang are with the School of Electrical and Computer Engineering, Georgia Institute of Technology, Atlanta, GA 30332, USA wwencen3, fumin@gatech.edu

[45]. Based on these work, we develop sufficient conditions for the cooperative H_∞ filter to admit feasible solutions and convergence.

In addition to theoretical analysis and computer simulations, experiments on real robots are necessary to verify our algorithms in a realistic environment with the presence of real-world uncertainties and variations that are not able to be considered beforehand. More specifically, for our cooperative exploration behavior, a realistic noisy field that is non-Gaussian is hard to be produced through simulation, which makes the experimental effort necessary. In addition, the theoretical bounds of the noise attenuation level of the cooperative H_∞ filter can be validated through experiments, which can enhance our understandings of the conservativeness of such bounds for real systems. Furthermore, the experiments can test the robustness of our strategy to communication delays in real life systems. Finally, experiments establish connections between biological systems and engineering systems in that the experimental data collected in both cases can be directly compared.

Our experiments are performed on a test-bed that includes a light field generated by an incandescent light bulb, a localization system, and several Khepera III robots [13]. The set-up shares similarities with multi-agent experimental test-beds documented in the literature [46]–[55]. The switching strategy for seeking the light source is implemented on the test-bed. In the experiments, we conduct several trials with respect to different memory lengths assigned to the robots, different formation sizes, and various noise attenuation levels for the cooperative H_∞ filter. We verify the influence of the memory length to the exploration behavior of the robots and justify the effects of different formation sizes and noise attenuation levels to the performance of the cooperative H_∞ filter.

Statement of contributions. In this paper, (1) we propose a switching strategy for a group of sensing agents to switch between individual exploration and cooperative exploration when exploring an unknown field, (2) we derive a cooperative H_∞ filter to provide estimates of field values and field gradients during cooperative exploration and prove sufficient conditions for the convergence and feasibility of the filter, and (3) we evaluate the strategy in realistic lab experiments.

The rest of the paper is organized as follows. Section II introduces the information dynamics for both individual exploration and cooperative exploration. Section III presents the formation shape and motion control for the agents in cooperative exploration. Section IV discusses the construction of the cooperative H_∞ filter and derives sufficient conditions for the feasibility and convergence of the filter. Section V proposes a switching strategy for a group of sensing agents to locate a local minimum of an unknown scalar field and introduces switching conditions from individual exploration to cooperative exploration and vice versa. Section VI describes the configuration of the multi-robot exploration test-bed and presents the experimental results. Section VII presents concluding remarks.

II. Information Dynamics

Let $z(\mathbf{r})$ be an unknown smooth scalar field perturbed by time-varying non-Gaussian noises where $\mathbf{r} \in \mathbb{R}^2$. N sensing agents are deployed in the field to perform an exploration task of seeking a local minimum. We assume that each agent can only take one measurement of the field at each time step and the agents can communicate with a central controller. The exploration behaviors of the group of sensing agents switch between two phases: individual exploration and cooperative exploration. In this section, we define the information dynamics for both phases.

A. Information Dynamics for Individual Exploration

Denote the position of the ith agent at kth time step as $\mathbf{r}_{i,k}$, the measurement taken by the ith agent as $p_{i,k}$ and the true field value at position $\mathbf{r}_{i,k}$ as $z_{i,k}$, where $i = 1, \cdots, N$. Then the measurement $p_{i,k}$ can be expressed as

$$p_{i,k} = z_{i,k} + v_{i,k}, \tag{1}$$

where $v_{i,k}$ represents the measurement noise whose statistical properties are assumed to be unknown.

To search for a local minimum, each agent moves in directions that may reduce the field value. For the sake of simplicity, we assume that each agent moves in the opposite direction of the gradient at its current position and the motion of each agent obeys the first order dynamics,

$$\dot{\mathbf{r}}_{i,k} = -\nabla \hat{z}_{i,k}, \tag{2}$$

where $\nabla \hat{z}_{i,k}$ is the estimated gradient of the field at the position $\mathbf{r}_{i,k}$. Note that equation (2) is not the only strategy that may lead to a local minimum. It is well known that biological entities such as the E. Coli switch between tumbling motion and straight line motion for gradient climbing [56]. The switching strategy developed in this paper does not depend on specific searching behaviors.

In the following, we give a simple example of estimating the gradient of the field $\nabla z_{i,k}$ by an individual agent at each time step k using the current and previous measurements. Note that $D_h z_{i,k} = \nabla z_{i,k} \cdot h$, where $D_h z_{i,k}$ is the directional derivative of the field at the position $\mathbf{r}_{i,k}$ in the direction h. If the successive positions of the agent are close enough, the gradient at the position $\mathbf{r}_{i,k}$ can be approximated by solving the following two equations.

$$p_{i,k} - p_{i,k-1} = \nabla \hat{z}_{i,k} \cdot (\mathbf{r}_{i,k} - \mathbf{r}_{i,k-1}), \tag{3}$$

$$p_{i,k-1} - p_{i,k-2} = \nabla \hat{z}_{i,k} \cdot (\mathbf{r}_{i,k-1} - \mathbf{r}_{i,k-2}). \tag{4}$$

If we define a matrix $\mathbf{R} = [\mathbf{r}_{i,k} - \mathbf{r}_{i,k-1}, \mathbf{r}_{i,k-1} - \mathbf{r}_{i,k-2}]^T$, then the solution to the above two equations is $\nabla \hat{z}_{i,k} = \mathbf{R}^{-1} \begin{pmatrix} p_{i,k} - p_{i,k-1} \\ p_{i,k-1} - p_{i,k-2} \end{pmatrix}$. If $\mathbf{r}_{i,k} - \mathbf{r}_{i,k-1} = \mathbf{r}_{i,k-1} - \mathbf{r}_{i,k-2}$, then $\mathbf{R}$ is singular and no valid estimates can be obtained by solving the above two equations. In this case, we let

$$\nabla \hat{z}_{i,k} = \frac{p_{i,k} - p_{i,k-1}}{\|\mathbf{r}_{i,k} - \mathbf{r}_{i,k-1}\|^2} (\mathbf{r}_{i,k} - \mathbf{r}_{i,k-1}) + \delta, \tag{5}$$

where δ is a small perturbation that prevents the agent from moving along a straight line so that equation (3) and equation

(4) will produce unique estimates of the field gradient. In the implementation of the algorithm, δ can be chosen as a Gaussian distributed random vector with zero mean and small variance.

B. Information Dynamics for Cooperative Exploration

In the cooperative exploration phase, the sensing agents need to remain in a formation and move in the field simultaneously. Therefore, we can treat the formation as a "super-agent" and consider its motion. Define the position of the formation center at kth step as $\mathbf{r}_{c,k}$ and the field value at the formation center as $z_{c,k}$. If $\mathbf{r}_{i,k}$ is close to $\mathbf{r}_{c,k}$, then we can use Taylor's expansion to approximate $z_{i,k}$. For $i = 1, \cdots, N$,

$$z_{i,k} \approx z_{c,k} + (\mathbf{r}_{i,k} - \mathbf{r}_{c,k})^T \nabla z_{c,k} + \frac{1}{2}(\mathbf{r}_{i,k} - \mathbf{r}_{c,k})^T \nabla^2 z_{c,k} (\mathbf{r}_{i,k} - \mathbf{r}_{c,k}), \tag{6}$$

where $\nabla z_{c,k}$ is the gradient of the field and $\nabla^2 z_{c,k}$ is the Hessian of the field at $\mathbf{r}_{c,k}$. Choose the state to be $\mathbf{s}_k = (z_{c,k}, \nabla z_{c,k}^T)^T$. When the center of the "super-agent" moves, the state evolves according to

$$\begin{aligned} z_{c,k} &= z_{c,k-1} + (\mathbf{r}_{c,k} - \mathbf{r}_{c,k-1})^T \nabla z_{c,k-1}, \\ \nabla z_{c,k} &= \nabla z_{c,k-1} + H_{c,k-1}(\mathbf{r}_{c,k} - \mathbf{r}_{c,k-1}), \end{aligned} \tag{7}$$

where $H_{c,k-1}$ is the estimate of the field Hessian $\nabla^2 z_{c,k-1}$.

Define $\mathbf{h}_{k-1} = (0, \mathrm{E}[H_{c,k-1}(\mathbf{r}_{c,k} - \mathbf{r}_{c,k-1})]^T)^T$ and $A_{k-1} = \begin{pmatrix} 1 & (\mathbf{r}_{c,k} - \mathbf{r}_{c,k-1})^T \\ 0 & \mathbf{I}_{3\times 3} \end{pmatrix}$, where E denotes the expectation with respect to the measurement noise in the process of estimating the field Hessian. We can see that A_{k-1} is nonsingular. Then the state equation can be expressed as

$$\mathbf{s}_k = A_{k-1}\mathbf{s}_{k-1} + \mathbf{h}_{k-1} + \mathbf{w}_{k-1}, \tag{8}$$

where $\mathbf{w}_{k-1}$ is a 3×1 noise vector that accounts for the noise in the field and the approximation error in the Taylor expansion. We assume that the statistic properties of $\mathbf{w}_{k-1}$ are unknown. Let C_k be a $N \times 3$ matrix with its ith row defined by $[1, (\mathbf{r}_{i,k} - \mathbf{r}_{c,k})^T]$ for $i = 1, 2, ..., N$ and D_k be a $N \times 4$ matrix with its ith row vector defined by the Kronecker product $\frac{1}{2}((\mathbf{r}_{i,k} - \mathbf{r}_{c,k}) \otimes (\mathbf{r}_{i,k} - \mathbf{r}_{c,k}))^T$. Define the $N \times 1$ measurement vector $\mathbf{p}_k = [p_{i,k}]$ and the noise vector $\mathbf{v}_k = [v_{i,k}]$ for $i = 1, \cdots, N$. We can write down the measurement equation as

$$\mathbf{p}_k = C_k \mathbf{s}_k + D_k \vec{H}_{c,k} + \mathbf{v}_k, \tag{9}$$

where $\vec{H}_{c,k}$ is the estimate of $H_{c,k}$ in a vector form, i.e., $\vec{H}_{c,k} = [H_{c,k(11)}\, H_{c,k(12)}\, H_{c,k(21)}\, H_{c,k(22)}]^T$. The estimation of the Hessian matrix $H_{c,k}$ is discussed in [7].

III. Formation Shape and Motion Control

In this section, we introduce the formation shape control and motion control of a group of agents when they are in the cooperative exploration phase.

We direct the center of the formation to follow the opposite direction of the field gradient estimate

$$\dot{\mathbf{r}}_{c,k} = -\nabla z_{c,k}. \tag{10}$$

Note that the gradient at any local minimum is zero. Therefore, once the formation center reaches a local minimum by moving along the opposite direction of the gradient, it will stay in the area containing the local minimum. The size of the area depends on the step size of movement.

The formation shape is described using Jacobi vectors $\mathbf{q}_{j,k}, j = 1, \cdots, N-1$ that satisfy $[\mathbf{r}_{c,k}, \mathbf{q}_{1,k}, \cdots, \mathbf{q}_{N-1,k}] = [\mathbf{r}_{1,k}, \mathbf{r}_{2,k}, \cdots, \mathbf{r}_{N,k}]\Psi$ where Ψ is the Jacobi transform. For example, if we deploy three agents, the Jacobi vectors are

$$\begin{aligned} \mathbf{q}_{1,k} &= \frac{\sqrt{2}}{2}(\mathbf{r}_{2,k} - \mathbf{r}_{3,k}), \\ \mathbf{q}_{2,k} &= \frac{\sqrt{6}}{6}(2\mathbf{r}_{1,k} - \mathbf{r}_{2,k} - \mathbf{r}_{3,k}), \end{aligned} \tag{11}$$

and the Jacobi transform $\Psi = \begin{pmatrix} \frac{1}{3} & \frac{1}{3} & \frac{1}{3} \\ 0 & \frac{\sqrt{2}}{2} & -\frac{\sqrt{2}}{2} \\ \frac{\sqrt{6}}{3} & -\frac{\sqrt{6}}{6} & -\frac{\sqrt{6}}{6} \end{pmatrix}$. The Jacobi transform decouples the kinetic energy of the entire system [7] [57], which enables us to design separate control laws for the formation center motion and the formation shape.

At step k, we apply the control laws

$$\mathbf{u}_{j,k} = -K_1(\mathbf{q}_{j,k} - \mathbf{q}_j^0) - K_2 \dot{\mathbf{q}}_{j,k}, j = 1, \cdots, N-1 \tag{12}$$

to $\ddot{\mathbf{q}}_{j,k} = \mathbf{u}_{j,k}$, where K_1 and K_2 are positive constant gains and $\mathbf{q}_j^0$ are designed vectors that define a desired formation. The control laws have an exponential rate of convergence. If we take the inverse Jacobi transform, then the new positions of the agents $\mathbf{r}_{i,k+1}, i = 1, \cdots, N$ can be obtained by

$$[\mathbf{r}_{1,k+1}, \mathbf{r}_{2,k+1}, \cdots, \mathbf{r}_{N,k+1}] = [\mathbf{r}_{c,k+1}, \mathbf{q}_{1,k+1}, \cdots, \mathbf{q}_{N-1,k+1}]\Psi^{-T}. \tag{13}$$

By applying the formation controller (12), the agents converge to a desired formation so that the cooperative exploration is achieved.

If there are obstacles presented in the field, obstacle avoidance algorithms should be incorporated into the motion planning equation (10) or equation (2) in the individual exploration phase. Since the formation motion control and formation shape control are decoupled, the formation shape control laws remain unchanged. In this paper, we focus on the switching behaviors between individual exploration and cooperative exploration. Therefore, we do not consider fields with obstacles. However, the strategy based on Jacobi Transforms can be extended to scenarios where there are obstacles [58].

IV. The Cooperative H_∞ Filter

In this section, we introduce the construction of the cooperative H_∞ filter that provides the estimates of field values and field gradients at the formation center in the cooperative exploration phase. Then we discuss the feasibility and convergence of the filter.

A. Construction of the Cooperative H_∞ Filter

Define a cost function J as the ratio between the energy of the estimation error and the energy of the disturbances

$$J = \frac{\sum_{k=0}^{M-1} \|\mathbf{s}_k - \hat{\mathbf{s}}_k\|_{Q_k}^2}{\|\mathbf{s}_0 - \hat{\mathbf{s}}_0\|_{P_0^{-1}}^2 + \sum_{k=0}^{M-1}(\|w_k\|_{W_k^{-1}}^2 + \|v_k\|_{V_k^{-1}}^2)}, \tag{14}$$

where $\hat{\mathbf{s}}_0$ is the initial estimate of $\mathbf{s}_0$, $P_0 > 0, Q_k \geq 0, W_k > 0$ and $V_k > 0$ are the weighting matrices chosen by design, which depend on the noise strengths. For example, we choose $W_k > V_k$ if we know that the sensor noise is stronger than the state noise. The goal of the H_∞ filter is to guarantee that the cost J is less than a prescribed noise attenuation level γ that can be expressed as $J < \gamma^2$.

Given the state equation (8) and the measurement equation (9), a cooperative H_∞ filter can be designed. Following the general steps of constructing the H_∞ filter [42], the equations of the cooperative H_∞ filter are as follows.

$$S_k = P_k^{-1} - \frac{1}{\gamma^2} Q_k + C_k^T V_k^{-1} C_k, \tag{15}$$

$$K_k = S_k^{-1} C_k^T V_k^{-1}, \tag{16}$$

$$\hat{s}_{k+1} = A_k \hat{s}_k + \mathbf{h}_k + A_k K_k (\mathbf{p}_k - C_k \hat{s}_k - D_k \vec{H}_{c,k}), \tag{17}$$

$$P_{k+1} = A_k S_k^{-1} A_k^T + W_k. \tag{18}$$

Note that the cooperative H_∞ filter can only be computed when the agents are in a formation and the performance of the cooperative H_∞ filter depends on the configurations of the formation.

B. Convergence and Feasibility of the Cooperative H_∞ Filter

The convergence of H_∞ filtering has been investigated for both continuous-time and discrete-time systems. Readers can refer to [38]–[41] and the references therein. The main feasibility results for discrete-time filtering are summarized in Theorem 4.1.

Theorem 4.1: Consider the system (8), (9) and the cost function (14). Under the condition that A_k is nonsingular for each k, an H_∞ filter guaranteeing an attenuation level γ exists between time $k = 0$ and $k = M$ if and only if there exist two sequences of positive definite matrices $\{S_k\}_{k=0}^{M-1}$ and $\{P_k\}_{k=0}^{M-1}$ such that

$$P_{k+1} = A_k S_k^{-1} A_k^T + W_k, \tag{19}$$

$$S_k = P_k^{-1} - \frac{1}{\gamma^2} Q_k + C_k^T V_k^{-1} C_k, \tag{20}$$

$$S_0 = P_0^{-1}, \tag{21}$$

$$S_k > 0, k = 0, 1, \cdots, M-1. \tag{22}$$

A feasible solution is defined as a positive definite solution P_k of the equation (19) that satisfies the equation (20).

The difference Riccati equation (DRE) (19) can also be written as

$$\begin{aligned} P_{k+1} &= A_k (P_k^{-1} - \frac{1}{\gamma^2} Q_k + C_k^T V_k^{-1} C_k)^{-1} A_k^T + W_k \\ &= A_k P_k A_k^T - A_k P_k [(C_k^T V_k^{-1} C_k - \frac{1}{\gamma^2} Q_k)^{-1} + P_k]^{-1} P_k A_k^T + W_k. \end{aligned} \tag{23}$$

As $k \to \infty$, if we drop the subscript ∞ for simplicity, then the Riccati equation (23) becomes

$$P = APA^T - AP[(C^T V^{-1} C - \gamma^{-2} Q)^{-1} + P]^{-1} PA^T + W. \tag{24}$$

The finite-horizon H_∞ problem becomes an infinite-horizon problem. If the solution to the infinite-horizon H_∞ filter exists, then the equation (24) admits a positive definite stabilizing solution P^s. In our case, since the noise properties of the field are unknown, we can select $Q_k \to \sigma_1^2 I, W_k \to \sigma_2^2 I$, and $V_k \to \sigma_3^2 I$, where I is the identity matrix. When $k \to \infty$, the formation is stabilized, then C goes to a constant matrix

$$C = \begin{pmatrix} 1 & (\mathbf{r}_1 - \mathbf{r}_c)^T \\ \vdots & \vdots \\ 1 & (\mathbf{r}_N - \mathbf{r}_c)^T \end{pmatrix} = \begin{pmatrix} 1 & \mathbf{d}_1^T \\ \vdots & \vdots \\ 1 & \mathbf{d}_N^T \end{pmatrix}, \tag{25}$$

where in 2D, $\mathbf{d}_i = [d_{i1}\ d_{i2}]^T$.

We now apply the feasibility and convergence conditions to the cooperative H_∞ filter and derive the sufficient conditions for the attenuation level and initial uncertainty that guarantee the convergence and feasibility of the cooperative H_∞ filter, which can give us a guidance in choosing γ and P_0 when implementing the filter. We have the following proposition.

Proposition 4.2: Assume that equation (24) admits a positive definite solution P^s. Starting from initial condition $0 < P_0 < P^s$, the solution P_k of the Riccati equation (23) at every step k exists and converges when $k \to \infty$. Moreover, if

(1) $\mathbf{r}_{c,k+1} - \mathbf{r}_{c,k} \to 0$ as $k \to \infty$, and

(2) the attenuation level γ satisfies

$$\begin{aligned} \gamma^2 > \max(0, &\frac{\sigma_1^2 \sigma_3^2}{N - |\sum_{i=1}^N d_{i1}| - |\sum_{i=1}^N d_{i2}|}, \\ &\frac{\sigma_1^2 \sigma_3^2}{\sum_{i=1}^N d_{i1}^2 - |\sum_{i=1}^N d_{i1}| - |\sum_{i=1}^N d_{i1} d_{i2}|}, \\ &\frac{\sigma_1^2 \sigma_3^2}{\sum_{i=1}^N d_{i2}^2 - |\sum_{i=1}^N d_{i2}| - |\sum_{i=1}^N d_{i1} d_{i2}|}), \end{aligned} \tag{26}$$

we obtain the solution that $P^s = \frac{1}{2}(\sigma_2^2 I + (\sigma_2^4 I + 4\sigma_2^2 X)^{\frac{1}{2}})$ where $X = (\sigma_3^{-2} C^T C - \sigma_1^2 \gamma^{-2} I)^{-1}$.

Proof: Let's first consider the solution P^s of the Riccati equation (24). Given the condition (1), we can approximate A_k by the identity matrix I. If we substitute $A = I$ into equation (24), then after rearranging terms, we can obtain

$$P^2 - \sigma_2^2 P - \sigma_2^2 (\sigma_3^{-2} C^T C - \sigma_1^2 \gamma^{-2} I)^{-1} = 0. \tag{27}$$

Define $X = (\sigma_3^{-2} C^T C - \sigma_1^2 \gamma^{-2} I)^{-1}$. Then the above equation can be written as $P^2 - \sigma_2^2 P - \sigma_2^2 X = 0$. For a quadratic matrix equation of the form

$$Q(Z) = A' Z^2 + B' Z + C' = 0, A', B', C' \in R^{n \times n}, \tag{28}$$

only when (1) $A' = I$, (2) B' and C' commute, and (3) the square root of $B'^2 - 4C'$ exists, we can apply the formula for the roots of a scalar quadratic equation and find a closed-form solution to the equation (28) [59]. The solution is $Z = \frac{1}{2}(-B' \pm (B'^2 - 4C')^{\frac{1}{2}})$. By comparison, $A' = I, B' = -\sigma_2^2 I$, and $C' = -\sigma_2^2 X$ satisfy the first two conditions. If the square root of $\sigma_2^4 I + 4\sigma_2^2 X$ exists, then we can get the solution as $P^s = \frac{1}{2}(\sigma_2^2 I + (\sigma_2^4 I + 4\sigma_2^2 X)^{\frac{1}{2}})$.

To check whether the square root of $\sigma_2^4 I + 4\sigma_2^2 X$ exists or not is equivalent to check whether $\sigma_2^4 I + 4\sigma_2^2 X$ is positive definite or not. From the facts that the identity matrix is positive definite and the sum of two positive definite matrices is positive definite, it is suffice to check the definiteness

of $X^{-1} = \sigma_3^{-2} C^T C - \sigma_1^2 \gamma^{-2} I$. We can compute that $C^T C = \begin{pmatrix} N & \sum_i^N \mathbf{d}_i^T \\ \sum_i^N \mathbf{d}_i & \sum_i^N \mathbf{d}_i \mathbf{d}_i^T \end{pmatrix}$. Plug $C^T C$ into X^{-1}, we have

$$X^{-1} = \begin{pmatrix} \sigma_3^{-2} N - \sigma_1^2 \gamma^{-2} & \sigma_3^{-2} \sum_i^N \mathbf{d}_i^T \\ \sigma_3^{-2} \sum_i^N \mathbf{d}_i & \sigma_3^{-2} \sum_{i=1}^N \mathbf{d}_i \mathbf{d}_i^T - \sigma_1^2 \gamma^{-2} I \end{pmatrix}. \tag{29}$$

We know that a symmetric matrix is positive definite if (1) all the diagonal entries are positive and (2) each diagonal entry is greater than the sum of the absolute values of all other entries in the same row. Therefore, we should have

$$\sigma_3^{-2} \sum_{i=1}^N d_{ij}^2 - \sigma_1^2 \gamma^{-2} > \sigma_3^{-2} |\sum_{i=1}^N d_{ij}| + \sigma_3^{-2} |\sum_{i=1}^N d_{i1} d_{i2}|, j = 1, 2. \tag{30}$$

and

$$\sigma_3^{-2} N - \sigma_1^2 \gamma^{-2} > \sigma_3^{-2} |\sum_{i=1}^N d_{i1}| + \sigma_3^{-2} |\sum_{i=1}^N d_{i2}|. \tag{31}$$

which yield

$$\gamma^2 > \frac{\sigma_1^2 \sigma_3^2}{N - |\sum_{i=1}^N d_{i1}| - |\sum_{i=1}^N d_{i2}|} > 0, \tag{32}$$

and

$$\gamma^2 > \frac{\sigma_1^2 \sigma_3^2}{\sum_{i=1}^N d_{ij}^2 - |\sum_{i=1}^N d_{ij}| - |\sum_{i=1}^N d_{i1} d_{i2}|} > 0, j = 1, 2. \tag{33}$$

Therefore, the matrix X^{-1} is positive if equation (26) is satisfied. This is the sufficient condition for our case so that we can get the solution P^s.

From Theorem 2 in [43], for some constant $\varepsilon > 0$ and the solution Y of a Lyapunov equation defined in [43], if $0 < P_0 < P^s + (Y + \varepsilon I)^{-1}$, then the solution P_k of equation (19) is feasible for all $k > 0$ and converges to the stabilizing solution P^s as $k \to \infty$. Since the matrix Y is positive definite, we can consider a stricter condition, which is $0 < P_0 < P^s$. Therefore, if $0 < P_0 < P^s$, the solution P_k to the Riccati equation (23) is feasible for all k and converges to the stabilizing solution P^s as $k \to \infty$. ■

Now let's consider a symmetric formation. Suppose the N agents are arranged so that $|\mathbf{d}_{i,k}| = a, i = 1, \cdots, N$, where a is a constant. Denote the phase angle of the vector $\mathbf{d}_{1,k}$ in the inertial frame by θ, and the angle between $\mathbf{d}_{i,k}$ and $\mathbf{d}_{1,k}$ by $\theta_i = \frac{2\pi}{N}(i-1)$. Then we can obtain $\mathbf{d}_{i,k} = a(\cos(\theta_i + \theta), \sin(\theta_i + \theta))^T$. We have the following corollary for the symmetric formation.

Corollary 4.3: Assume that equation (24) admits a positive definite solution P^s. For a symmetric formation, starting from initial condition $0 < P_0 < P^s$, the solution P_k of the Riccati equation (23) at every step k exists and converges when $k \to \infty$. Moreover, if

(1) $\mathbf{r}_{c,k+1} - \mathbf{r}_{c,k} \to 0$ as $k \to \infty$, and

(2) the attenuation level γ satisfies

$$\gamma^2 > \max(\frac{\sigma_1^2 \sigma_3^2}{N}, \frac{2\sigma_1^2 \sigma_3^2}{aN}), \tag{34}$$

we obtain the solution that

$$P^s = \frac{1}{2} diag(\sigma_2(\sigma_2^2 + \frac{4\gamma^2}{\sigma_3^{-2}\gamma^2 N - \sigma_1^2})^{\frac{1}{2}} + \sigma_2^2, \sigma_2(\sigma_2^2 + \frac{8\gamma^2}{a\sigma_3^{-2}\gamma^2 N - 2\sigma_1^2})^{\frac{1}{2}} + \sigma_2^2, \sigma_2(\sigma_2^2 + \frac{8\gamma^2}{a\sigma_3^{-2}\gamma^2 N - 2\sigma_1^2})^{\frac{1}{2}} + \sigma_2^2). \tag{35}$$

Proof: When the formation is symmetric, we use the following relationships,

$$\sum_{i=1}^N \mathbf{d}_i = a \sum_{i=1}^N (\cos(\theta_i + \theta), \sin(\theta_i + \theta))^T = \mathbf{0}, \tag{36}$$

$$\sum_{i=1}^N d_{i1}^2 = a^2 \sum_{i=1}^N \cos^2(\theta_i + \theta) = \frac{1}{2} a^2 N, \tag{37}$$

$$\sum_{i=1}^N d_{i2}^2 = a^2 \sum_{i=1}^N \sin^2(\theta_i + \theta) = \frac{1}{2} a^2 N, \tag{38}$$

$$\sum_{i=1}^N d_{i1}^2 d_{i2}^2 = a^2 \sum_{i=1}^N \cos(\theta_i + \theta) \sin(\theta_i + \theta) = 0. \tag{39}$$

Therefore, we can obtain that $X = diag(\sigma_3^{-2} N - \sigma_1^2 \gamma^{-2}, \frac{1}{2} a \sigma_3^{-2} N - \sigma_1^2 \gamma^{-2}, \frac{1}{2} a \sigma_3^{-2} N - \sigma_1^2 \gamma^{-2})^{-1}$. In order to obtain $X > 0$, we should have $\gamma^2 > \max(\frac{\sigma_1^2 \sigma_3^2}{N}, \frac{2\sigma_1^2 \sigma_3^2}{aN})$. If we plug X into $P^s = \frac{1}{2}(\sigma_2^2 I + (\sigma_2^4 I + 4\sigma_2^2 X)^{\frac{1}{2}})$ obtained in Proposition 4.2, we can obtain the equation (35). The rest of the proof is similar to the proof of Proposition 4.2. ■

Remark: The condition (1) in Proposition 4.2 and Corollary 4.3 is satisfied if the formation center eventually stops moving. If the source seeking strategy is successful, then this condition will be satisfied since the formation center will stay near a local minimum of the field.

Proposition 4.2 and Corollary 4.3 imply that a lower noise attenuation level γ and a smaller error bound P^s can be achieved as the number of agents increases and the formation gets larger. The choices of γ and P_0 also depend on the noise strength, which requires users to have some preliminary knowledge of the field before running the filter.

V. The Switching Strategy

Having obtained the information dynamics for both individual exploration and cooperative exploration, we are in the position of discussing the switching between these two phases. In the individual exploration phase, if the switching conditions are satisfied, the agents switch to cooperative exploration. In the cooperative exploration phase, the agents send measurements to a central controller that runs a cooperative H_∞ filter and provides the new positions of the agents. If the agents detect that the noise level reduces to a certain extent, they switch back to individual exploration. The flowchart of the switching strategy is illustrated in Fig. 1.

A. Individual Exploration to Cooperative Exploration

In the individual exploration phase, the agents estimate the field gradient utilizing the time-series measurements. If the

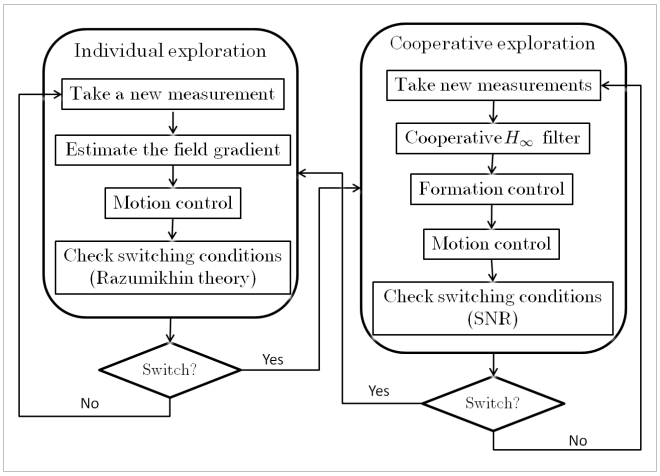

Fig. 1. The flowchart of the switching strategies.

noise level gets higher, the estimates of the gradient directions will become more noisy, which may prevent the agents from finding the right direction. Therefore, we propose a switching condition based on the Razumikhin theorem for the agents to check whether they can keep individual exploration and find a local minimum.

We first restate the Razumikhin theorem for the asymptotic stability of time-delay systems [16] without proof.

Theorem 5.1: (Razumikhin) *Given a system* $\dot{x}(t) = f(t, x_t)$ *where* $x \in \mathbb{R}^n$ *and* $x_t \in \mathscr{C}$ *represents the delayed system trajectory, suppose* $f : \mathbb{R} \times \mathscr{C} \to \mathbb{R}^n$ *takes bounded subsets of* $\mathscr{C}$ *into bounded subsets of* $\mathbb{R}^n$. *Suppose* $\alpha_1, \alpha_2, w : \mathbb{R}_+ \to \mathbb{R}_+$ *are continuous nondecreasing functions,* $\alpha_1(u) > 0$, $\alpha_2(u) > 0$ *and* $w(u) > 0$ *for* $u > 0$, *and* $\alpha_1(0) = \alpha_2(0) = 0$, α_2 *strictly increasing. Suppose there exists a continuous nondecreasing function* $g(u) > u$ *for* $u > 0$. *If there exists a continuous differentiable function* $V : \mathbb{R} \times \mathbb{R}^n \to \mathbb{R}$ *such that*

$$\alpha_1(\|x(t)\|) \leq V(t, x(t)) \leq \alpha_2(\|x(t)\|), \forall t \in \mathbb{R}, x \in \mathbb{R}^n, \quad (40)$$

and the derivative of V *along the solution* $x(t)$ *satisfies*

$$\dot{V}(t, x(t)) \leq -w(\|x(t)\|), \quad (41)$$

whenever $V((t+\theta), x(t+\theta)) \leq g(V(t, x(t)))$ *for all* $\theta \in [-r, 0]$, *then the equilibrium* $x(t) = 0$ *of the system is asymptotically stable.*

For discrete systems, condition (41) becomes [14]

$$V(k+1, x(k+1)) - V(k, x(k)) \leq -w(\|x(k)\|), \quad (42)$$

whenever $V((k+\theta), x(k+\theta)) \leq g(V(k, x(k)))$ for all $\theta \in [-r, 0]$.

Now consider a single sensing agent. For simplicity, we drop the subscript i used to index the agent in the following arguments. We suppose that the agent has a memory with finite length r, where $r \in \mathbf{Z}^+$. The memory is used to store the measurements p_{k+s} where s is a non-positive integer such that $-r \leq s \leq 0$. Based on the discrete time Razumikhin theorem, we have the following proposition.

Proposition 5.2: Suppose the field value z_k *satisfy* $z_{\min} \leq z_k \leq z_{\max}, \forall k$. *Let* $\bar{p}_k = \max_{s \in [-r,0]} p_{k+s}$ *where* $r \in \mathbf{Z}^+$ *and* p_k *is the measurement at time step* k. *If* $p_{k+1} - p_k \leq -\rho p_k + \rho z_{\min}$ *whenever* $(1+\varepsilon)p_k \geq \bar{p}_k + \varepsilon z_{\min}$, *where* $\rho, \varepsilon > 0$ *are infinitesimal constants, then* p_k *will converge to* $z_{\min}$ *as* $k \to \infty$.

Proof: Define a new variable $y_k = p_k - z_{min} \geq 0$ so that $y_{max} = z_{max} - z_{min}$ and $0 \leq y_k \leq y_{max}$. Let $V(y_k) = y_k \in [0, y_{max}]$. Define $\bar{y}_k = \max_{s \in [-r,0]} y_{k+s}$. If we choose $g(V(y_k)) = (1+\varepsilon)y_k$, where $\varepsilon > 0$ is an infinitesimal constant, then the condition $V(\bar{y}_k) \leq g(V(y_k))$ in the Razumikhin theorem becomes $\max_{s \in [-r,0]} y_{k+s} \leq (1+\varepsilon)y_k$. The condition can be rewritten as $\max_{s \in [-r,0]}(p_{k+s} - z_{\min}) \leq (1+\varepsilon)(p_k - z_{min})$. If we further simplify the condition, we can obtain:

$$\bar{p}_k + \varepsilon z_{\min} \leq (1+\varepsilon)p_k. \quad (43)$$

On the other hand, we have $V(y_{k+1}) - V(y_k) = p_{k+1} - p_k$. Choose $w(y_k) = \rho y_k = \rho p_k - \rho z_{\min}$, where ρ is another infinitesimal constant. According to the Razumikhin theorem, if for all $k \in [r, \infty)$, the measurements satisfy $p_{k+1} - p_k \leq -\rho p_k - \rho z_{\min}$ whenever $(1+\varepsilon)p_k \geq \bar{p}_k + \varepsilon z_{\min}$, then y_k converge to 0 as $k \to \infty$. This fact implies that p_k converge to $z_{\min}$ as $k \to \infty$. ■

Given the above proposition, we propose the following exploration algorithm for individual exploration.

Algorithm 5.3: Suppose an agent is searching for a local minimum of an unknown field, where the field value satisfies $z_{\min} \leq z_k \leq z_{\max}$. Let $\bar{p}_k = \max_{s \in [-r,0]} p_{k+s}$, where r is the memory length of the agent.

(1) At step $k \geq r$, the agent takes a measurement of the field p_k. Then estimates the field gradient ∇z_k by solving the equations (3) and (4).

(2) The agent moves in the opposite direction of the estimated gradient according to $\dot{\mathbf{r}}_k = -\nabla \hat{z}_k$ or uses other strategies to reduce the measured field value. At step $k+1$, the agent takes a new measurement p_{k+1}.

(3) At step $k+1$, the agent checks whether $(1+\varepsilon)p_k \geq \bar{p}_k + \varepsilon z_{\min}$ is satisfied or not. If yes, the agent checks the value of $p_{k+1} - p_k$. If $p_{k+1} - p_k \leq -\rho p_k + \rho z_{\min}$, it keeps individual exploration. Otherwise, it requires to switch to cooperative exploration. If for all $k > 0$, $p_{k+1} - p_k \leq -\rho p_k + \rho z_{\min}$ whenever $(1+\varepsilon)p_k \geq \bar{p}_k + \varepsilon z_{\min}$, the agent will converge to a local minimum $z_{\min}$ according to Proposition 5.2.

According to Proposition 5.2 and Algorithm 5.3, the switching conditions from individual exploration to cooperative exploration can be stated as: (1) at time step $k+1$, check if $(1+\varepsilon)p_k \geq \bar{p}_k + \varepsilon z_{\min}$. If (1) is satisfied, then (2) check if $p_{k+1} - p_k > -\rho p_k + \rho z_{\min}$. Once an agent detects that both switching conditions are satisfied at step $k+1$, it notifies other agents, then all agents switch to cooperative exploration upon request. This ensures that all agents behave consistently in the cooperative exploration phase.

B. Cooperative Exploration to Individual Exploration

According to the information dynamics for cooperative exploration introduced in Section II-B, when all the agents are moving in a formation, which is treated as a "super-agent", a cooperative H_∞ filter is producing estimates of field values and gradients at the formation center. Then the convergence

of the cooperative exploration algorithm is dictated by the same sufficient conditions for convergence of the individual exploration algorithm. Define $\bar{z}_{c,k} = \max_{s\in[-r_c,0]} z_{c,k+s}$, where r_c is the memory length of the "super-agent" that can be considered as the average of the memory lengths of all the individual agents in the formation. For simplicity and without loss of generality, we assume that all the agents have the same memory lengths. As long as (1) $(1+\varepsilon)z_{c,k} \geq \bar{z}_{c,k} + \varepsilon z_{\min}$ and (2) $z_{c,k+1} - z_{c,k} > -\rho z_{c,k} + \rho z_{\min}$ are not satisfied, the formation will converge to a local minimum of the field. However, there exist fields that cooperative exploration will fail. We find that the success of an exploration mission is related to the noise level, the sensor resolution, and the step size of the moving agents [60]. Further investigation of such field will be performed in future works.

One reason that the collaborating sensing agents outperform individual agents is that at each step, the H_∞ filter provides the filtered field value by combining measurements from N agents, which serves as an effective way of noise reduction while a single agent can only make use of the time-series measurements with no reduction of noises. When the field is time-varying and the noise level reduces to the extent that a single agent is able to generate accurate gradient estimates, the cooperative sensing agents should break out the formation and start individual exploration again.

We utilize the signal-to-noise ratio (SNR) to serve as the switching condition from cooperative exploration to individual exploration. If we define the signal-to-noise ratio obtained by the ith agent at the step k as

$$\beta_{i,k} = 10\log_{10} \sum_{\xi=0}^{r} \frac{\hat{p}_{i,k-\xi}^2}{(p_{i,k-\xi} - \hat{p}_{i,k-\xi})^2}, i = 1, \cdots, N. \qquad (44)$$

where $\hat{p}_{i,k}$ is the estimated field value obtained by

$$\hat{p}_{i,k} = z_{c,k} + (\mathbf{r}_{i,k} - \mathbf{r}_{c,k})^T \nabla z_{c,k}, \qquad (45)$$

then we have the following algorithm for the agents to decide when to switch from cooperative exploration back to individual exploration.

Algorithm 5.4: Define the average SNR at time step k as $\bar{\beta}_k = \frac{1}{N}\sum_{i=1}^{N} \beta_{i,k}$. Suppose that at time T_s, the agents have switched to cooperative exploration. Then for $k > T_s + r_c$, where r_c is the memory length of the super agent, the cooperative agents switch back to individual exploration if $\bar{\beta}_k > \mu \bar{\beta}_{T_s+r_c}$, where $\mu > 1$ is a constant.

The constant μ is chosen by design. A larger μ tends to prevent the agents from switching to individual exploration since the SNR needs to increase by a large amount to satisfy Algorithm 5.4. If μ is small, the agents switch to individual exploration as soon as they detect the noise reduces by a small amount. However, if the agents can not individually converge to a field minimum, they have to switch back to cooperative exploration again, which increases the exploration effort and cost. If that happens, one may increase μ so that a larger threshold can be set.

VI. Experiments

To evaluate our switching strategy for exploration, we design a multi-agent exploration test-bed consisting of a group of mobile robots performing source seeking tasks. In this section, we introduce the configuration of the test-bed and discuss the experimental results.

A. Experimental test-bed

Fig. 2 shows the experimental test-bed that includes several components:

1) Robots and sensors: We choose Khepera III robots from K-Team to implement the switching strategy. Khepera III is a round mobile robot running on two differential drive wheels and a sliding support. Each Khepera III robot has nine infra-red (IR) sensors placed around it and two infra-red ground sensors placed on the bottom. We use the nine IR sensors around the robot to measure the ambient light intensity. The sensor readings are normalized to be within the range $[0, 5000]$. The higher the light intensity is, the **lower** the sensor reading is.

2) Localization system: As seen in Fig. 2, the localization system consists of an overhead camera, a camera support and the LabVIEW vision system for providing the positions and orientations of the robots at each time step.

3) Central computer: A central controller is running on a central computer in the cooperative exploration phase. At each time step, the localization system obtains the new positions and orientations of the robots and the robots collect new measurements of the field. These information are sent to the central computer. Then the central computer calculates the new positions and orientations of the robots at the next step and sends the corresponding moving distances and turning angles back to the robots. All these communications are performed wirelessly. In the individual exploration phase, since the robots are searching the field on their own, the central computer does nothing but receives the positions and orientations of the robots from the localization system.

4) Light field: We use a standard 40W incandescent light bulb to serve as a light source that generates a light field unknown to the robots. The field is about 2.8 meters long and 1.6 meters wide. The light intensity decreases when the distance from the light source increases, which indicates that the location of the light bulb hosts the maximum of the intensity of the light field. Therefore, seeking for the maximum of the light field corresponds to finding the minimum of the measured field.

B. Experimental Results

Since the field minimum is unknown to the robots and $\rho > 0$ and $\varepsilon > 0$ in Algorithm 5.3 are infinitesimal constants, we approximate ρ and ε by 0 so that the condition $p_{k+1} - p_k \leq -\rho p_k + \rho z_{\min}$ whenever $(1+\varepsilon)p_k \geq \bar{p}_k + \varepsilon z_{\min}$ is simplified to $p_{k+1} - p_k < 0$ whenever $p_k > \bar{p}_k$. If we consider the derivation from the Razumikhin theorem to Proposition 4.2, the simplified condition corresponds to the Razumikhin theorem on stability, not asymptotic stability. Therefore, under the simplified condition, the agents can only be guaranteed to stay near a local minimum, not converge to a local minimum. In the experiments, because of the disturbances and noises in the field and measuring process, we still observe the

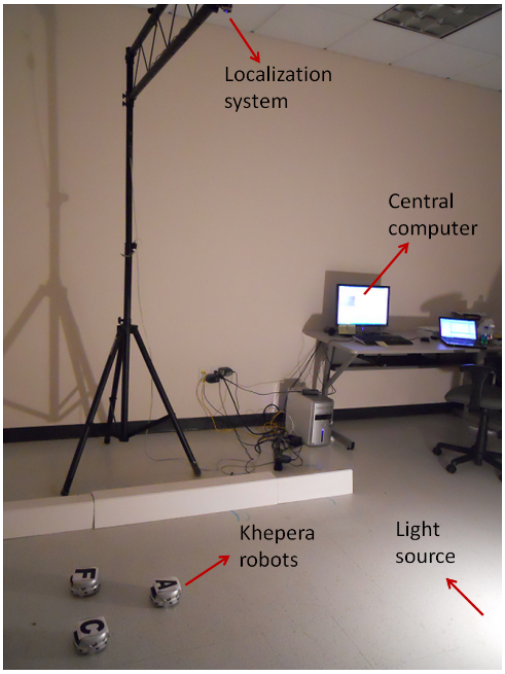

Fig. 2. The experimental setting.

convergence to the field minimum, which is not surprising since the conditions in the Razumkhin Theorem is sufficient but not necessary.

We deploy three Khepera III robots in the light field, which are labeled as "A", "F" and "C", respectively. Fig. 3 shows the trajectories of the three robots searching for the light source with the switching strategy from one trial with the memory length $r = 5$. The information collected are plotted in Fig. 4, in which the green (solid with dot marker), red (dashed with dot marker), and yellow (dotted with dot marker) lines indicate the measurements taken by robots A, F, and C, respectively and the blue line (dashed with triangular marker) indicates the filtered field values at the formation center after they switched to cooperative exploration. At first few steps, each robot explores the field independently. After several steps, individual exploration is abandoned because of high noise strength, then they switch to cooperative exploration and find the light source.

In this experiment, at step $k = 13$, robot A detects that $p_{13} > \max_{s\in[-5,0]} p_{13+s}$. According to the switching conditions from individual exploration to cooperative exploration, the robot needs to check if $p_{14} > p_{13}$ at step 14. At step $k = 14$, the robot takes a new measurement and detects that $p_{14} > p_{13}$. In this case, the switching conditions in Algorithm 5.3 are satisfied and robot A decides to switch to cooperative exploration. It sends a switching signal to the central computer through wireless connection and the central computer broadcasts a signal to all the robots once it received the switching signal from robot A. Due to the communication delay, at step $k = 16$, all the robots receive the signal from the central computer and start to cooperate. Since we do not actively control the existing noises, the robots never detect that the field noise level decreases to the extent that they can switch back to individual exploration. They keep exploring the field cooperatively and locate the field minimum in around 50 steps. Other parameters in these experiments are as follows: the formation size $a = 0.2$m, the noise attenuation level $\gamma = 3$, the weighting matrices $Q = I$, $W = 0.01I$, and $V = 0.01I$.

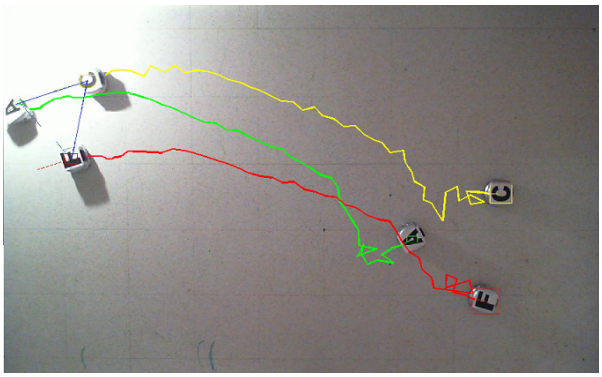

Fig. 3. Trajectories of three robots seeking for the light source with the switching strategy.

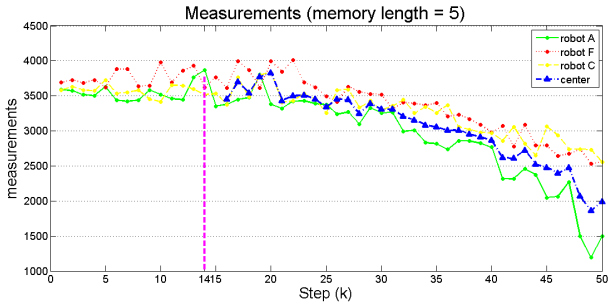

Fig. 4. Measurements when memory length is 5. At step $k = 16$, the robots switch to cooperation.

1) Effects of the memory length r: To illustrate the influence of the memory length on the exploration behavior of the robots, we conduct other two experiments with different memory lengths. Fig. 5 and Fig. 6 show the measurements corresponding to the memory lengths 10 and 20. As seen in Fig. 5, at step $k = 27$, robot F checks that the switching conditions are satisfied and at the same step the robots switch to cooperative exploration. In around 60 steps, the robots reach the light source. In Fig. 6, the memory length $r = 20$. At step $k = 57$, robot A sends out the switching signal to the central computer and at step $k = 58$, the robots switch to cooperative exploration. They take around 80 steps to find the light source.

The three trials with different memory lengths indicate that the memory length r plays an important role in the switching strategy. For a given field, if the noise level is high so that it is hard for the robots to find the source by themselves, the shorter the memory length is, the earlier the robots realize the situation and switch to cooperative exploration. On the other hand, a longer memory indicates higher noise tolerance. In situations that the cooperative exploration cost is high so that it is preferable for robots to explore the field individually, longer memory lengths give more chances to the robots to explore the field by their own.

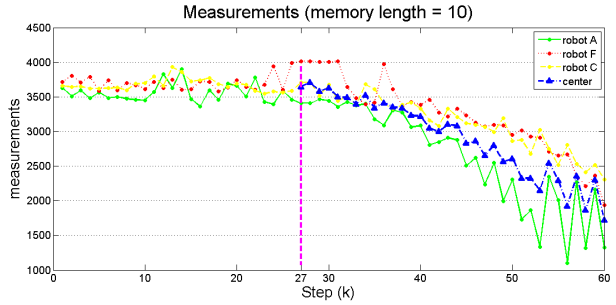

Fig. 5. Measurements when memory length is 10. At step $k = 27$, the robots switch to cooperation.

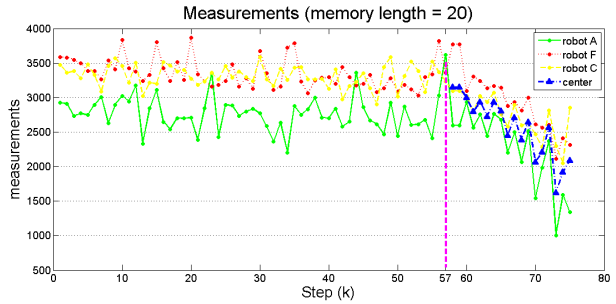

Fig. 6. Measurements when memory length is 20. At step $k = 57$, the robots switch to cooperation.

Fig. 7 shows the measurements taken by one robot in another experiment. In this trial, the memory length is set to be 60, which is long enough for the robot not to switch to cooperative exploration. We can see from the figure that even though the measurements are noisy, since the switching conditions are not satisfied with $r = 60$, the robot is able to find the light source after around 100 steps, which verifies the fact we discussed previously that as long as the switching conditions are not satisfied, a robot moves towards a local minimum of a field.

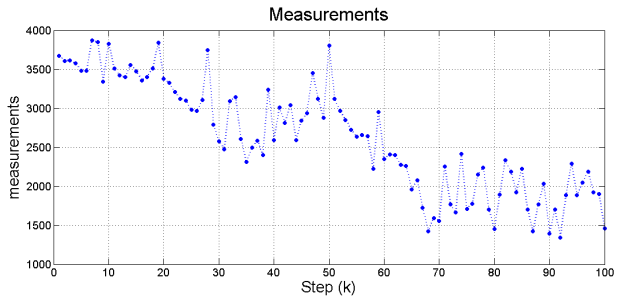

Fig. 7. Measurements taken by one robot with memory length $r = 60$ but doesn't switch.

2) Effects of the noise attenuation level γ: Fig. 8 illustrates the traces of the error bound P_k of the H_∞ filter associated with different noise attenuation levels when the robots are in the cooperative exploration phase. In these experiments, we also set $a = 0.2$m, $Q = I$, $W = 0.01I$, and $V = 0.01I$. Given the parameters and from the sufficient conditions (26), we can calculate that if $\gamma^2 > \max(\frac{\sigma_1^2\sigma_3^2}{N}, \frac{2\sigma_1^2\sigma_3^2}{aN}) = \max(\frac{0.01}{3}, \frac{2\times 0.01}{0.2\times 3}) = 0.033$, which implies $\gamma > 0.1826$, then the cooperative H_∞ filter will converge. In Fig. 8, we can see that, when $\gamma > 0.1826$, the noise bound P_k converges to a steady state value P^s. Actually, since (26) is only a sufficient condition for convergence, when $\gamma < 0.1826$, the cooperative H_∞ filter may converge as well. We have tested that when $\gamma > 0.045$, the cooperative H_∞ filter converges. Only when $\gamma < 0.045$, the cooperative H_∞ filter becomes unstable.

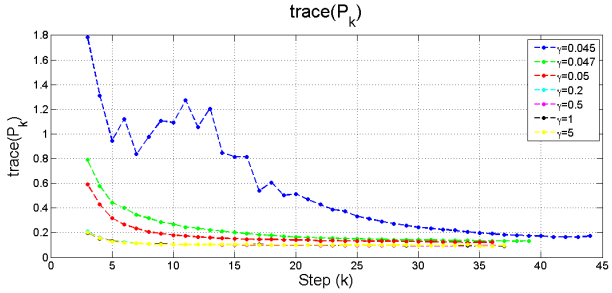

Fig. 8. Trace(P_k) when the noise attenuation level of the H_∞ filter γ varies.

3) Effects of the formation size a: Fig. 9 illustrates the trace of the error bound P_k of the H_∞ filter associated with different formation sizes when the robots are in the cooperative exploration phase. In these experiments, we set the noise attenuation level $\gamma = 3$, the weighting matrices $Q = I$, $W = 0.01I$, and $V = 0.01I$. Equation (35) also indicates that as the formation size a increases, the trace of P^s decreases. We can clearly see the tendency in Fig. 9.

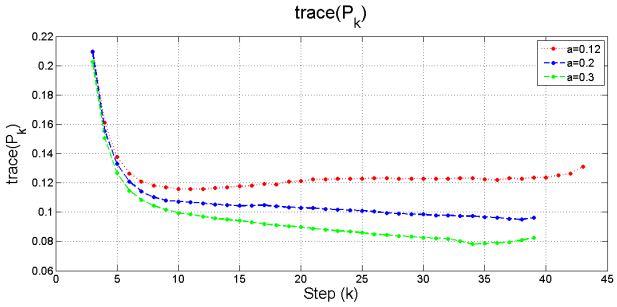

Fig. 9. Trace(P_k) when the distance between each pair of the robots varies.

4) Comparison with purely individual exploration: As we discussed before, Fig. 7 shows the measurements taken by one robot without switching to cooperative exploration. We can also consider this experiment as the robot exploring the field with purely individual exploration strategy. As we can see from the figure, the convergence rate is slower compared to the experiment with switching strategy, as shown in Fig. 4, Fig. 5, and Fig. 6. Therefore, with the switching strategy, we can achieve a higher rate of convergence.

5) Comparison with purely cooperative exploration: Fig. 10 shows the measurements taken by three robots in an experiment with purely cooperative exploration strategy. The settings are the same as the experiments we introduced before with the formation size $a = 0.35m$. As illustrated in the figure, the formation formed by the robots converges to the light source in fewer steps. However, since cooperative exploration is associated with increased cost such as communication and

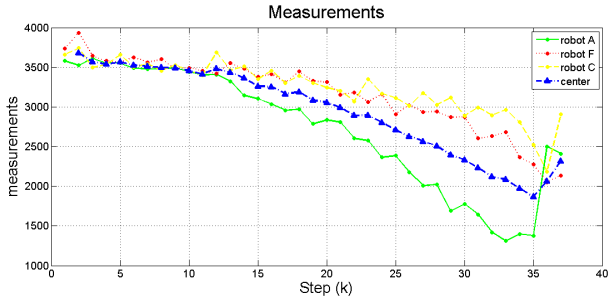

Fig. 10. Measurements taken by three robots with purely cooperative exploration.

computation, in fields with lower noise levels, the switching strategy can allow the agents to seek the source individually without collaborating if the switching conditions are not satisfied. Thus, the cost can be reduced.

C. Complementary Simulation Results

In the experiments, once the robots switch to cooperative exploration, they do not switch back to individual exploration because the noises are not under our control and remain at a constant level. To justify our switching condition from cooperative exploration to individual exploration, we simulate three sensing agents searching for a minimum of a two dimensional scalar field that is corrupted by time-varying uniformly distributed noises. The field is generated according to $z = (x-10)^2 + 2(y-10)^2$. We assume that at step $k = 80$, the noise level in the field increases from 5% to 30% and at step $k = 250$, the noise level reduces from 30% to 5%. We choose the memory length $r = 20$ in algorithm 1 and $\mu_1 = 1.3$ in algorithm 3.

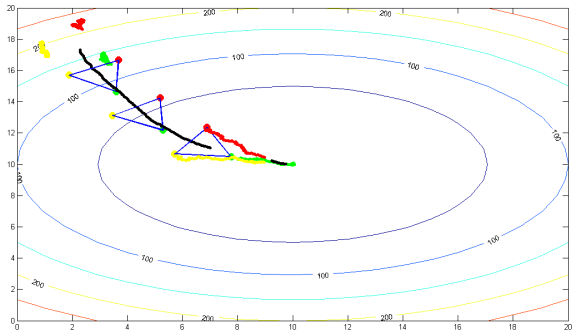

Fig. 11. The trajectories of the sensing agents. The green, red, and yellow lines indicate the trajectories of the agents in the individual exploration phase and the black line indicates the trajectory of the formation center in the cooperative exploration phase.

Fig. 11 illustrates the exploration process of the three sensing agents. The agents form a symmetric formation. The colored lines are trajectories of the three agents when they are performing individual exploration. The black line is the trajectory of the formation center when the agents are collaborating. Fig. 12 shows the filtered field values measured by each agent with different colored lines corresponding to different

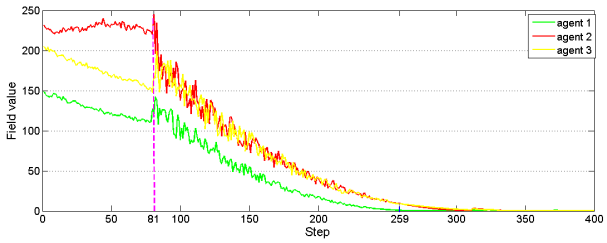

Fig. 12. Measurements taken by the agents. The agents switch to cooperative exploration at $k = 81$ and switch back to individual exploration at $k = 259$.

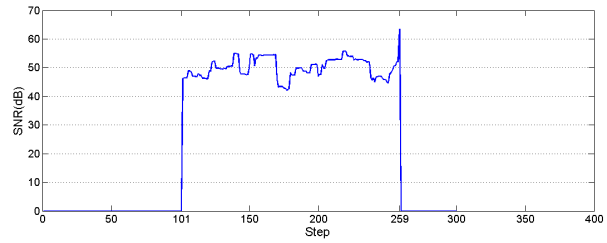

Fig. 13. The average signal-to-noise ratio. When $k > 101$ and $k < 259$, the agents calculate the SNR. After $k = 259$, the agents switch back to individual exploration.

agents in Fig. 11. Fig. 13 shows the estimated SNR when the agents are performing cooperative exploration. The figures indicate that the agents start from individual exploration. At step $k = 86$, they switch to cooperative exploration. Thus, $T_s = 86$. When $k > T_s + r = 106$, the SNR is computed and at $k = 259$, the agents find that $\bar{\beta}_k > 1.3\bar{\beta}_{T_s+r}$, so they switch back to individual exploration and succeed in locating the field minimum in around 300 steps.

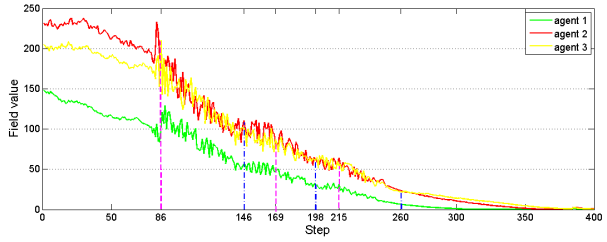

Fig. 14. Measurements taken by the agents. The agents switch to cooperative exploration at $k = 86, 169$, and 215 and switch back to individual exploration at $k = 146, 198$, and 260.

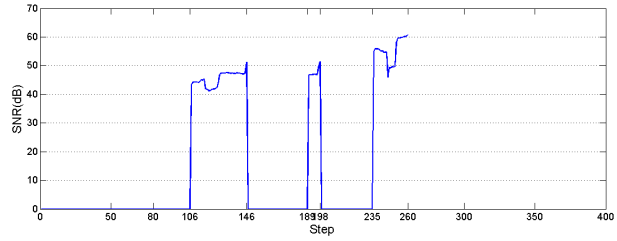

Fig. 15. The average signal-to-noise ratio.

If we set μ_1 to be a smaller value and keep other settings the same as the first simulation, we can observe from the simula-

tion results that the switchings between individual exploration and cooperative exploration happen several times during one trial. Fig. 14 indicates the measurements taken by the agents. In this simulation, we choose $\mu_1 = 1.1$ and $\varepsilon = 0.05$. The agents switch to cooperative exploration at $k = 86, 169$, and 215 and switch back to individual exploration at $k = 146, 198$, and 260. Fig. 15 shows the corresponding SNR calculated in this trial. In this simulation, the agents take around 400 steps to converge to the field minimum. We can see that the larger μ_1 tends to keep the agents in the cooperative exploration phase and increase the rate of convergence of the exploration behavior.

VII. Conclusions

We develop a strategy for a group of agents that seek for a local minimum in an unknown scalar field efficiently by switching between individual exploration and cooperative exploration. Based on the Razumikhin theorem, we propose algorithms for each agent to decide whether to switch to cooperative exploration. The switching from cooperative exploration to individual exploration is based on the change of the signal-to-noise (SNR) ratio. In the cooperative exploration phase, a cooperative H_∞ filter is constructed to produce estimates of field values and field gradients. We rigorously justify the convergence and feasibility of the cooperative H_∞ filter.

A multi-agent test-bed is developed for testing cooperative exploration tasks. We implement the switching strategy on the test-bed and observe from the experiments that

1) Given a noisy field, robots with shorter memory lengths switch to cooperative exploration earlier than robots with longer memory lengths. Longer memory lengths have higher tolerance to noises while shorter memory lengths help the robots to start cooperation earlier.
2) Our switching strategy is robust to realistic communication delays.
3) The conservative theoretical bound of the noise attenuation level γ is verified.
4) The error bound of the cooperative H_∞ filter reduces when the formation size increases.

In our future work, we will compare engineering data collected from the robots with the biological data collected from fish groups.

References

[1] R. Simmons, D. Apfelbaum, W. Burgard, D. Fox, M. Moors, S. Thrun, and H. Younes, "Coordination for multi-robot exploration and mapping," in *Proc. 17th National Conference on Artificial Intelligence. 12th Innovative Applications of Artificial Intelligence Conference (IAAI-2000)*, 2000, pp. 852–858.

[2] P. Ogren, E. Fiorelli, and N. E. Leonard, "Cooperative control of mobile sensor networks: Adaptive gradient climbing in a distributed environment," *IEEE Transactions on Automatic Control*, vol. 49, no. 8, pp. 1292–1302, 2004.

[3] J. Clark and R. Fierro, "Cooperative hybrid control of robotic sensors for perimeter detection and tracking," in *Proc. of 2005 American Control Conference*, 2005, pp. 3500 – 3505.

[4] B. Grocholsky, J. Keller, V. Kumar, and G. Pappas, "Cooperative air and ground surveillance," *IEEE Robotics and Automation Magazine*, vol. 13, no. 3, pp. 16–25, 2006.

[5] S. Susca, S. Martínez, and F. Bullo, "Monitoring environmental boundaries with a robotic sensor network," *IEEE Transactions on Control Systems Technology*, vol. 16, no. 2, pp. 288–296, 2008.

[6] R. Graham and J. Cortes, "Cooperative adaptive sampling via approximate entropy maximization," in *Proc. of 48th IEEE Conf. on Decision and Control*, Shanghai, China, 2009, pp. 7055–7060.

[7] F. Zhang and N. E. Leonard, "Cooperative control and filtering for cooperative exploration," *IEEE Transactions on Automatic Control*, vol. 55, no. 3, pp. 650–663, 2010.

[8] Y. Cao, A. Fukunaga, and A. Khang, "Cooperative mobile robotics: Antecedents and directions," *Autonomous Robots*, vol. 4, no. 1, pp. 7–27, 1997.

[9] G. Dudek, M. Jenkin, E. Milios, and D. Wilkes, "A taxonomy for multiagent robotics," *Autonomous Robots*, vol. 3, no. 4, pp. 375–397, 1996.

[10] R. Bachmayer and N. E. Leonard, "Vehicle networks for gradient descent in a sampled environment," in *Proc. of 41st IEEE Conf. on Decision and Control*. IEEE, 2002, pp. 113–117.

[11] C. Torney, Z. Neufeld, and L. Couzin, "Context-dependent interaction leads to emergent search behavior in social aggregates," *Proc. of the National Academy of Sciences*, vol. 106, no. 52, pp. 22 055–22 060, 2009.

[12] W. Wu and F. Zhang, "A switching strategy for robust cooperative exploration," in *Proc. of 2010 IEEE Conf. on Decision and Control*, 2010, pp. 5493–5498.

[13] ——, "Experimental validation of source seeking with a switching strategy," in *IEEE Conference on Robotics and Automation*, 2011, pp. 3835–3840.

[14] S. Elaydi and S. Zhang, "Stability and periodicity of difference equations with finite delay," *Funkcialaj Ekvacioj*, vol. 37, pp. 401–413, 1994.

[15] S. Zhang and M. Chen, "A new Razumikhin theorem for delay difference equations," *Computers & Mathematics with Applications*, vol. 36, pp. 10–12, 1998.

[16] K. Gu, V. L. Kharitonov, and J. Chen, *Stability of Time-Delay Systems*. Boston: Birkhäuser, 2003.

[17] M. Krstic and H. H. Wang, "Stability of extremum seeking feedback for general nonlinear dynamic systems," *Automatica*, vol. 36, pp. 595–601, 2000.

[18] Y. Tan, D. Nesic, and I. M. Y. Mareels, "On non-local stability properties of extremum seeking control," *Automatica*, vol. 42, pp. 889–903, 2006.

[19] C. Manzie and M. Krstic, "Extremum seeking with stochastic perturbations," *IEEE Transactions on Automatic Control*, vol. 54, pp. 580–585, 2009.

[20] M. Stankovic and D. Stipanovic, "Extremum seeking under stochastic noise and applications to mobile sensors," *Automatica*, vol. 46, pp. 1243–1251, 2010.

[21] C. G. Mayhew, R. G. Sanfelice, and A. R. Teel, "Robust hybrid source-seeking algorithms based on directional derivatives and their approximations," in *Proc. of 47th IEEE Conf. Decision and Control*, 2008, pp. 1735–1740.

[22] A. Matveev, H. Teimoori, and A. V. Savkin., "Navigation of a nonholonomic vehicle for gradient climbing and source seeking without gradient estimation," in *Proc. of 2010 American Control Conference*, 2010, pp. 219 – 223.

[23] E. Burian, D. Yoerger, A. Bradley, and H. Singh, "Gradient search with autonomous underwater vehicles using scalar measurements," in *Proceedings of the 1996 Symposium on Autonomous Underwater Vehicle Technology*, 1996, pp. 86 – 98.

[24] J. A. Farrell, P. Shuo, and W. Li, "Chemical plume tracing via an autonomous underwater vehicle," *IEEE Journal of Oceanic Engineering*, vol. 30, no. 2, pp. 428–442, 2005.

[25] Y. Li, M. A. Rotea, G. T.-C. Chiu, L. G. Mongeau, and I.-S. Paek, "Extremum seeking control of a tunable thermoacoustic cooler," *IEEE Transactions on Control Systems Technology*, vol. 13, no. 4, pp. 527–536, 2005.

[26] X. T. Zhang, D. M. Dawson, W. E. Dixon, and B. Xian, "Extremum-seeking nonlinear controllers for a human exercise machine," *IEEE/ASME Transactions on Mechatronics*, vol. 11, no. 2, pp. 233–240, 2006.

[27] J. Cochran and M. Krstic, "Nonholonomic source seeking with tuning of angular velocity," *IEEE Transactions on Automatic Control*, vol. 54, no. 4, pp. 717–731, 2009.

[28] H. Ishida, Y. Kagawa, T. Nakamoto, and T. Moriizumi, "Odor-source localization in the clean room by an autonomous mobile sensing system," *Sensors and Actuators, B: Chemical*, vol. 32, no. 2, pp. 115–121, 1996.

[29] A. Martins, J. Almeida, and E. Silva, "Coordinated maneuver for gradient search using multiple AUVs," in *Proc. of OCEANS 2003*, vol. 1, 2003, pp. 347 – 352.

[30] Y. Liu and K. Passino, "Stable social foraging swarms in a noisy environment," *IEEE Transactions on Automatic Control*, vol. 49, no. 1, pp. 30–40, 2004.
[31] D. Zarzhitsky, D. F. Spears, and W. M. Spears, "Swarms for chemical plume tracing," in *Proc. IEEE Swarm Intelligence Symp. SIS 2005*, 2005, pp. 249–256.
[32] R. D. Robinett and D. G. Wilson, "Collective plume tracing: A minimal information approach to collective control," in *Proc. of 2007 American Control Conference*, 2007, pp. 4884–4891.
[33] W. Jatmiko, Y. Ikemoto, T. Matsuno, T. Fukuda, and K. Sekiyama, "Distributed odor source localization in dynamic environment," in *Proc. IEEE Sensors*, 2005.
[34] V. Gazi, "Swarm aggregations using artificial potentials and sliding-mode control," *IEEE Transactions on Robotics*, vol. 21, no. 6, pp. 1208 – 1214, 2005.
[35] N. E. Leonard, D. A. Paley, F. Lekien, R. Sepulchre, D. M. Fratantoni, and R. E. Davis, "Collective motion, sensor networks, and ocean sampling," *Proceedings of the IEEE*, vol. 95, no. 1, pp. 48–74, 2007.
[36] J. Cortes, "Distributed gradient ascent of random fields by robotic sensor networks," in *Proc. 46th IEEE Conf. on Decision and Control*, 2007, pp. 3120–3126.
[37] E. Biyik and M. Arcak., "Gradient climbing in formation via extremum seeking and passivity-based coordination rules," in *Proc. of 46th IEEE Conf. on Decision and Control*, 2007, pp. 3133–3138.
[38] I. Yaesh and U. Shaked, "A transfer function approach to the problem of discrete-time systems: H_∞ optimal linear control and filtering," *IEEE Transactions on Automatic Control*, vol. 36, pp. 1264–1271, 1991.
[39] K. M. Nagpal and P. P. Khargonekar, "Filtering and smoothing in a H_∞ setting," *IEEE Transactions on Automatic Control*, vol. 36, pp. 152–166, 1991.
[40] I. Yaesh and Y. Theodor, "H_∞ optimal estimation: a turtorial," in *Proc. of 31st IEEE Conf. on Decision and Control*, Tucson, Arizona, 1992, pp. 2278–2286.
[41] Y. Theodor, U. Shaked, and C. Souza, "A game theory approach to robust discrete-time H_∞ estimation," *IEEE Transactions on Signal Processing*, vol. 42, no. 6, pp. 1486–1495, 1994.
[42] D. Simon, *Optimal State Estimation*. Hoboken, New Jersey: Wiley-Interscience, 2006.
[43] P. Bolzern, P. Colaneri, and G. D. Nicolao, "Transient and asymptotic analysis of discrete-time H_∞ filters," *European Journal of Control*, vol. 3, pp. 317–324, 1997.
[44] P. Bolzern and M. Maroni, "New conditions for the convergence of H_∞ filters and predictors," *IEEE Transactions on Automatic Control*, vol. 44, pp. 1564–1568, 1999.
[45] A. H. Sayed, "A framework for state-space estimation with uncertain models," *IEEE Transactions on Automatic Control*, vol. 46, no. 7, pp. 998–1013, 2001.
[46] A. Martinoli, A. J. Ijspeert, and F. Mondada, "Understanding collective aggregation mechanisms: From probabilistic modelling to experiments with real robots," *Robotic and Autonomous Systems*, vol. 29, pp. 51–63, 1999.
[47] M. J. B. Krieger, J. B. Billeter, and L. Keller, "Ant-like task allocation and recruitment in cooperative robots," *Nature*, vol. 406, no. 6799, pp. 992–995, 2000.
[48] R. Bachmayer and N. Leonard, "Experimental test-bed for multi-vehicle control, navigation and communication." in *Proc. 12th Int. Symp. Unmanned Untethered Submersible Tech*, 2001.
[49] L. Cremean, W. B. Dunbar, D. Gogh, J. Hickey, E. Klavins, J.Meltzer, and R. M. Murray, "The Caltech multi-vehicle wireless testbed," in *Proc. of 41st IEEE Conf. on Decision and Control*, 2002, pp. 86–88.
[50] Z. Jin, S. Waydo, and E. B. Wildanger, "MVWT-II: the second generation Caltech multi-vehicle wireless testbed," in *Proc. of 2004 American Control Conference*, 2004, pp. 5321–5326.
[51] C. H. Hsieh, Z. Jin, D. Marthaler, B. Q. Nguyen, D. J. Tung, A. L. Bertozzi, and R. M. Murray, "Experimental validation of an algorithm for cooperative boundary tracking," in *Proc. of 2005 American Control Conference*, 2005, pp. 1078–1083.
[52] D. Cruz, J. McClintock, B. Perteet, O. A. A. Orqueda, C. Yuan, and R. Fierro, "Decentralized cooperative control: a multivehicle platform for research in networked embedded systems," *IEEE Control Systems Magazine*, vol. 27, no. 3, pp. 58–78, 2007.
[53] N. Michael, J. Fink, and V. Kumar., "Experimental testbed for large multi-robot teams: Verification and validation," *IEEE Robotics and Automation Magazine*, vol. 15, no. 1, pp. 53–61, 2008.
[54] A. Joshi, T. Ashley, Y. Huang, and A. L. Bertozzi, "Experimental validation of cooperative environmental boundary tracking with on-board sensors," in *Proc. of 2009 American Control Conference*, St. Louis, MO, 2009, pp. 2630–2635.
[55] W. Ren, H. Chao, W. Bourgeous, N. Sorensen, and Y. Chen, "Experimental validation of consensus algorithms for multivehicle cooperative control," *IEEE Transactions on Control Systems Technology*, vol. 16, no. 4, pp. 745–752, 2008.
[56] H. C. Berg, *E. Coli in motion*. New York: Springer, 2004.
[57] F. Zhang, "Geometric cooperative control of particle formations," *IEEE Transactions on Automatic Control*, vol. 55, no. 3, pp. 800–803, 2010.
[58] F. Zhang and S. Haq, "Boundary following by robot formations without gps," in *Proc. IEEE Int. Conf. Robotics and Automation*, 2008, pp. 152–157.
[59] N. J. Higham and H. Kim, "Numerical analysis of a quadratic matrix equation," *IMA Journal of Numerical Analysis*, vol. 20, pp. 499–519, 2000.
[60] W. Wu and Fumin, "Explorability of noisy scalar fields," in *Proc. 2011 IEEE International Conference on Decision and Control*, 2011, pp. 6439–6444.

Wencen Wu Wencen Wu received her B.S. and M.S. degrees from the School of Electronic, Information and Electrical Engineering at Shanghai Jiao Tong University, Shanghai, China, in 2006 and 2009, respectively, and her M.S. degree from the School of Electrical and Computer Engineering at the Georgia Institute of Technology, Atlanta, USA, in 2010, where she is currently pursuing a Ph.D. degree. Her research interests include bio-inspired autonomy, cooperative control, and multi-robot exploration.

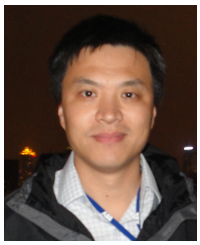

Fumin Zhang Fumin Zhang received the B.S. and M.S. degrees from Tsinghua University, Beijing, China, in 1995 and 1998, respectively, and the Ph.D. degree from the Department of Electrical and Computer Engineering, University of Maryland, College Park, in 2004. He has been an Assistant Professor in the School of ECE, Georgia Institute of Technology since 2007. He was a Lecturer and Postdoctoral Research Associate in the Mechanical and Aerospace Engineering Department, Princeton University from 2004 to 2007. His research interests include marine autonomy, mobile sensor networks, and theoretical foundations for battery supported cyber-physical systems. He received the NSF CAREER Award in 2009, and the ONR YIP Award in 2010.